

## Article

# Mix Design and Field Detection of Large-Particle-Size Graded Crushed Stone Mixtures for Pavement Reconstruction

Qigui Yi <sup>1</sup>, Jie Xu <sup>2</sup>, Haoyu Pan <sup>3</sup>, Xinchao Lv <sup>3</sup>, Kuiyuan Xiong <sup>3</sup> and Xuelian Li <sup>2,\*</sup> 

<sup>1</sup> Guidong Highway Development Center, Wuzhou 543000, China; ylk027181@126.com

<sup>2</sup> School of Traffic and Transportation, Changsha University of Science and Technology, Changsha 410114, China; 21101030095@csust.edu.cn

<sup>3</sup> Guangxi Transportation Science and Technology Group Co., Ltd., Nanning 530007, China; haoyu\_pan@163.com (H.P.); xinchao\_lv@163.com (X.L.); xj928594709@163.com (K.X.)

\* Correspondence: lixuelian@csust.edu.cn

**Abstract:** Large-particle-size graded crushed stone mixtures (LPS-GCSMs) can improve the shortcomings of conventional graded crushed stone, such as low strength, high deformation, and a low modulus of resilience. At present, there is no systematic research on the gradation design and field evaluation of the LPS-GCSMs. In this study, compaction and California bearing ratio (CBR) tests and field construction conditions were combined to design six kinds of gradation of LPS-GCSM, and the optimum gradation was revealed. In order to improve the mechanical properties of LPS-GCSM, 2.5% cement was added to the mixture to prepare a low-content cement-modified LPS-GCSM (LCC-LPS-GCSM) based on the suggested gradation. The mechanical properties of the LCC-LPS-GCSM were investigated through unconfined compression strength (UCS) and compression rebound modulus (CRM) tests. Moreover, the compaction and deflection properties of LPS-GCSM and LCC-LPS-GCSM were examined through the test battery. The results showed that the optimum gradation of LPS-GCSM can be achieved with a combination of aggregate sizes of 20–40 mm, 10–20 mm, 5–10 mm, and 0–5 mm at a ratio of 44:20:10:26. The passing rates of 19 mm and 4.75 mm should be approximately at the median value of the gradation in view of field construction uniformity and a coarse aggregate interlocking effect. The UCS and CRM values of LCC-LPS-GCSM increased rapidly from 0 day to 28 days while they slowed after 28 days, which was similar to those of cement-stabilized materials. The field detection suggested that LPS-GCSM exhibited favorable compaction and that the addition of cement improved the stability of the field compaction of the mixture. Adding a subbase course of LPS-GCSM between the old pavement and the LCC-LPS-GCSM base can lead to more uniform stress on the base. The results of this study provide a reference for the gradation design of LPS-GCSM and optimization of the design indicators.

**Keywords:** large-particle-size graded crushed stone; mix design; California bearing ratio; degree of compaction; deflection



**Citation:** Yi, Q.; Xu, J.; Pan, H.; Lv, X.; Xiong, K.; Li, X. Mix Design and Field Detection of Large-Particle-Size Graded Crushed Stone Mixtures for Pavement Reconstruction. *Buildings* **2024**, *14*, 1359. <https://doi.org/10.3390/buildings14051359>

Academic Editor: Pengfei Liu

Received: 8 April 2024

Revised: 5 May 2024

Accepted: 8 May 2024

Published: 10 May 2024



**Copyright:** © 2024 by the authors. Licensee MDPI, Basel, Switzerland. This article is an open access article distributed under the terms and conditions of the Creative Commons Attribution (CC BY) license (<https://creativecommons.org/licenses/by/4.0/>).

## 1. Introduction

Graded crushed stone (GCS) is a kind of mixture composed of coarse aggregates, fine aggregates, and sand in certain proportions [1]. As a kind of granular material without binders, GCS has the advantages of easy access to its raw materials, low cost, and convenient construction [2]. In addition, an excellent effect of stress dissipation can be achieved through the application of GCS in a pavement structure [3]. When GCS is used between the semi-rigid base and the asphalt mixture surface course, it can disperse the concentrated stresses, reduce the generation of reflective cracks, and provide support for the pavement structure [4,5]. Moreover, due to its large void ratio, GCS can also be used as a drainage course of asphalt pavements to accelerate the moisture drainage, thus reducing the water damage to pavements and extending the service life of the road [6]. Therefore, GCS is widely used for the base or subbase of asphalt pavements worldwide [7–9].

However, when conventional GCS is used for the base of asphalt pavements, permanent deformation under repeated traffic loads is prone to occurring, which easily leads to structural rutting, fatigue cracking, and other pavement failures [10,11]. This is because the strength of GCS is mainly formed by internal friction resistance and bonding forces [12]. The maximum aggregate size of conventional GCS is relatively small, so it is difficult to form a dense skeleton structure among aggregates [13]. As a result, conventional GCS is characterized by low strength, high plastic deformation, and a low modulus of resilience [14]. Previous studies have shown that the California bearing ratio (CBR), dynamic modulus of resilience, and permeability of GCS can be significantly increased with an increase in the maximum particle size, which can reduce pavement distress and the cost of pavement maintenance [15,16]. Moreover, the Illinois Department of Transportation has found that the performance of GCS is significantly affected by the gradation design method. GCS with a large size of aggregates is more resistant to freezing and thawing than conventional GCS [17,18]. Eustacchio et al. discovered that GCS with a large size of aggregates was more stable and had a higher compressive capacity than conventional GCS [19]. Furthermore, GCS with a maximum particle size of 53 mm cannot only form an interlocking skeleton structure with a high bearing capacity and durability but also has a better drainage effect [20].

Currently, there is no defined mix design method for a large-particle-size graded crushed stone mixture (LPS-GCSM) in Chinese specifications or those of other countries. The Guangxi Zhuang Autonomous Region of China has formulated a local standard, the "Technical Specification for Construction of Large Size Graded Crushed Stone Base" based on the application of LPS-GCSM in construction. According to this specification, the nominal maximum particle size of LPS-GCSM is 53 mm, and the proportion of coarse particles above 19 mm should not be less than 40%. In addition, some related preliminary investigations into the mix design method of the LPS-GCSM have been conducted by researchers. Tan et al. proposed a gradation design method based on the skeleton-dense structure of LPS-GCSM, which combined the Talbol theory and the *i*-method [21]. The passing rate of each sieve for coarse aggregates and fine aggregates was calculated by the Talbol method and *i*-method, respectively. The levels of gradation calculated by the Talbol method and *i*-method were then combined to obtain various sets of gradation compositions. It was found that the mixture with a gradation of  $n = 0.55$  and  $i = 0.70$  had the best mechanical properties in laboratory tests [22]. Luo determined the key sieves of LPS-GCSM based on the planar three-circle stacking theory, Bailey theory, and SAC gradation method [23]. Based on the skeleton-dense structure of the mixture, Suo et al. adopted the Bailey method to identify the key sieves for LPS-GCSM and determined the key sieve passing rate. Then, the Fuller formula was utilized to calculate the passing rate of sieves except for the key sieves. Finally, the VCADRF method was used to examine whether the gradation was interlocking [24]. Guo et al. employed the particle interference theory and Talbol method to design the gradation of LPS-GCSM and determine the optimum gradation [25]. To achieve the closest packing of particles and a dense structure of the mixture, Ding et al. designed the gradation of LPS-GCSM with the maximum particle size of 73 mm, based on the graded filling theory and the particle interference theory. Moreover, the Bailey method was used to optimize the gradation [26]. Yuan et al. applied the compressive packing model to the gradation optimization of LPS-GCSM. According to the characterization of the skeleton structure, it was concluded that 13.2 mm and 26.5 mm were the key sieve sizes, which were 0.22 and 0.5 times the maximum particle size, respectively [27].

In addition, the field applications of LPS-GCSM have also been studied in China. Shi et al. found that reconstructed pavement with the LPS-GCSM base could effectively prevent the occurrence of reflective cracks in the test road [28]. Xia et al. carried out a series of experiments, including the quality control of raw materials, gradation design, construction quality control, and mechanical properties in several pavement reconstruction projects, and asserted that the LPS-GCSM base had a more stable interlocking skeleton structure, better deformation resistance, and better pavement performance than the traditional base [29].

Long and Zhou et al. evaluated the resilient modulus of old asphalt pavement with an LPS-GCSM base by using the field bearing plate method, and they suggested that the LPS-GCSM base had a higher modulus and better resistance to heavy loads than the conventional GCS base [30,31]. Based on these findings, it can be seen that LPS-GCSM exhibits an excellent pavement performance on construction sites and has promising application prospects.

In summary, LPS-GCSM shows excellent physical and mechanical properties, but there are no uniform design methods for LPS-GCSM. Most of the existing design methods for LPS-GCSM are only based on laboratory tests and fail to consider field construction characteristics. Therefore, in this study, the gradation of LPS-GCSM was designed and optimized through a series of laboratory and field experiments, and then the designed gradation was examined on test roads. Firstly, laboratory tests and field constructions were carried out to design LPS-GCSM and determine the optimum gradation. Then, in order to improve the mechanical properties of LPS-GCSM, 2.5% cement was added to the mixture to prepare low-content cement-modified LPS-GCS (LCC-LPS-GCSM) with the designed gradation. The basic mechanical properties of LCC-LPS-GCSM were also tested. The designed gradation was finally examined through the compaction and deflection of the test road. The results of this study provide a reference for the gradation design of LPS-GCSM and a theoretical basis for the promotion and application of an LPS-GCS flexible base.

## 2. Research Objective and Methodology

The objective of this study was to investigate the gradation design method and pavement performance of LPS-GCSM. The following methodology was adopted to achieve the objective of this study:

(1) Six kinds of gradation were designed, and they were optimized by compaction and CBR tests to determine the target gradation.

(2) On the basis of the designed gradation, the target gradation was modified by considering variations in raw materials and the uniformity of field paving.

(3) Cylindrical specimens of LCC-LPS-GCS were prepared and cured under standard curing conditions for 1 day, 7 days, 28 days, and 90 days. Unconfined compression strength (UCS) and compression rebound modulus (CRM) tests were conducted to investigate the mechanical properties of LCC-LPS-GCS.

(4) Compaction and deflection tests were conducted for the base and subbase of the test road to examine the designed gradation.

## 3. Raw Materials and Experimental Program

### 3.1. Coarse Aggregate

The coarse aggregate used in this study was limestone obtained from a quarry in Shanglin County, Nanning City, Guangxi Zhuang Autonomous Region, China. The coarse aggregates were divided into three sets, which were 20–40 mm, 10–20 mm, and 5–10 mm. According to the Chinese specification JTG E42-2005 [32], the technical indicators of the coarse aggregate were tested. All indicators and corresponding results are shown in Table 1, and all results meet the requirements of the specification JTG/T F20-2015 [33].

**Table 1.** Basic properties of the coarse aggregate.

Technical Indicator	Unit	Technical Requirement	20–40 mm	Test Results 10–20 mm	5–10 mm
Mud content	%	≤1.0	0.5	0.1	0.5
Clod content	%	≤0.5	0.1	0.1	0.2
Needle flake content	%	≤20.0	12.6	13.8	-
Crushing value	%	≤25.0	13.7	14.2	-
Apparent density	g/cm <sup>3</sup>	≥2500	2735	2724	2714
Bulk density	g/cm <sup>3</sup>	≥1350	1642	1631	1612
Water absorption	%	≤3.0	0.38	0.47	0.57
Void ratio	%	≤47	39.6	39.9	39.5

### 3.2. Fine Aggregate

The properties of fine aggregate have a significant impact on the water stability of the LPS-GCSM. Fine aggregate should be dry, clean, free of weathering, free of impurities, and have an appropriate particle gradation. In addition, the passing rate of the 0.075 mm sieve should be  $\leq 15\%$  to ensure that the mixture possesses a high level of water permeability and enables water to drain quickly. The fine aggregate for this research was limestone, and the properties of the fine aggregate were tested based on the Chinese specification JTG E42-2005 [32]. All test results are shown in Table 2, which comply with the requirements of specification JTG/T F20-2015 [33].

**Table 2.** Basic properties of the fine aggregate.

Property	Unit	Technical Requirement	Test Result
Mud content	%	$\leq 5$	2.1
Clod content	%	$\leq 5$	1.2
Sand equivalent	%	$\geq 55$	69
Mica content	%	$\leq 2.0$	1.1
Crushing value	%	$\leq 25.0$	17.5
Liquid limit	%	$\leq 28$	19.5
Plasticity index	-	$< 6$	3.5
Apparent density	g/cm <sup>3</sup>	$\geq 2500$	2646
Bulk density	g/cm <sup>3</sup>	$\geq 1400$	1482
Apparent relative density	g/cm <sup>3</sup>	$\geq 2450$	2532
Porosity	%	$\leq 45.0$	19.8

### 3.3. Cement

Polenta cement (P.O 42.5) was selected in this study. According to the test methods in Chinese specification JTG 3420-2020 [34], the properties of the cement were examined, and the test results are summarized in Table 3. All the results complied with the requirements for cement in Chinese specification JTG/T F20-2015 [33].

**Table 3.** Characteristics of the cement.

Property	Measured Value	Unit	Technical Requirement
Density	3.08	g/cm <sup>3</sup>	-
Normal consistency	28.4	%	-
Specific surface area	340	cm <sup>2</sup> /kg	$\geq 300$
Setting time	Initial setting		$\geq 180$
	Final setting		$\geq 360$ and $\leq 600$
Compressive strength	3 d	MPa	$\geq 3.5$
	28 d	MPa	$\geq 6.5$
Rupture strength	3 d	MPa	$\geq 17$
	28 d	MPa	$\geq 42.5$

### 3.4. Compaction Test

Compared to conventional GCS, the maximum particle size of LPS-GCSM is larger and the content of particles above 40 mm is higher. Due to the limitation on the maximum particle size of a test cylinder in the Chinese specification [35], these specimens are difficult to prepare and the results need to be corrected if the conventional compaction method is applied, which leads to a significant error in the test results. Therefore, the surface vibration compaction method was adopted in this study, which is used with a larger test cylinder and can improve the compaction effect and physical and mechanical properties of specimens [36]. This is because the vibration compaction method provides a better orientation of the aggregate particles, which leads to the formation of well-structured mixtures and reduces the accumulation of plastic deformation [37,38].

The compaction test referred to the T 0133-2019 surface vibration compactor method in Chinese specification JTG 3430-2020 [35]. The type of surface vibration instrument used

in this test was BZYS-4212 (shown in Figure 1), with a power of 0.75~2.2 kW, a vibration frequency of 30~50 Hz, and an excitation force of 10~80 kN, which can produce a static pressure of more than 18 kPa on the surface of the specimen. The inner diameter and height of the test cylinder were 280 mm and 230 mm, respectively. Before the test, the prepared materials were mixed well, and they were added to the test cylinder in three equal portions. The time of each vibration was set as 6 min, and the height of the specimen was measured when the compaction was completed (shown in Figure 2).



**Figure 1.** The surface vibration instrument.



**Figure 2.** The measurement of the specimen height.

The maximum dry density of the mixture was calculated according to the following equation.

$$\rho_{d\max} = \frac{M_d}{A_c H} \quad (1)$$

where  $\rho_{d\max}$  is the maximum dry density ( $\text{g}/\text{cm}^3$ );  $M_d$  is the mass of dry mixtures (g);  $A_c$  is the cross-sectional area of the test cylinder ( $\text{cm}^2$ ); and  $H$  is the height of the vibration compaction specimen (cm).

### 3.5. California Bearing Ratio Test

The California bearing ratio (CBR) is an index proposed by the State of California to evaluate the deformation resistance of the road base and pavement materials [39]. Deformation resistance is characterized by the ability of the material to resist the deformation of a partial load. The CBR test is convenient and the equipment is economical; therefore, it is widely adopted in many countries.

In this study, the CBR test referred to T 0134-2019 in Chinese specification JTG 3430-2020 [35]. A fully automatic digital display pavement material strength tester (PMS) was used to conduct penetration experiments; the type of instrument was CH-128C, with a maximum bearing capacity of 200 kN (shown in Figure 3). The CBR specimens were prepared using the vibration compaction apparatus. There were three replicates for each

gradation. Then, the porous plate was placed on the upper end of the prepared specimen and four load plates (5 kg in total) were placed on the porous plate. All specimens were then immersed in water for 4 days before the test, as shown in Figure 4.

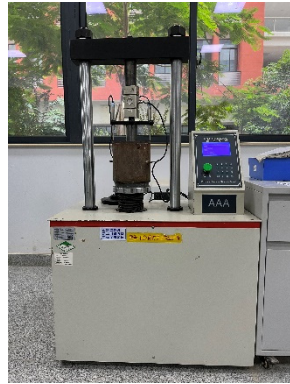


**Figure 3.** The pavement material strength tester.



**Figure 4.** The CBR specimens.

The immersed specimens were placed on the PMS for penetration experiments. The diameter and length of the penetration rod were 50 mm and 100 mm, respectively. The bearing ratios for penetrations of 2.5 mm and 5 mm could be calculated according to Equations (2) and (3), and the larger value of these two was chosen as the final result.

$$CBR = \frac{p}{7000} \times 100 \quad (2)$$

$$CBR = \frac{p}{10,500} \times 100 \quad (3)$$

where  $CBR$  is the bearing ratio of the specimen (%); and  $p$  is pressure (kPa).

### 3.6. Unconfined Compressive Strength Test

UCS tests are carried out by a PMS, and the detailed process refers to Chinese specification T 0805-1994 in JTG E51-2009 [40]. Thirteen replicate specimens were tested for each cement content. The specimens with curing completed were placed on the PMS. Then, a load with a rate of 1 mm/min was applied to the specimens, and the maximum pressure  $P$  at the time of damage was recorded. The following equation is used to calculate the UCS values.

$$R = \frac{4P}{\pi D^2} \quad (4)$$

where  $R$  is the UCS value of the specimen (MPa);  $P$  is the maximum pressure of damage (N); and  $D$  is the diameter of the specimen (mm).

### 3.7. Compressive Resilient Modulus Test

CRM tests are also carried out by the PMS, with reference to T 0808-1994 in Chinese specification JTG E51-2009 [40]. Thirteen replicate specimens were tested for each cement content. Before the test, the specimens with completed curing were smoothed on both sides with cement mortar and placed in water for 24 h. After the water immersion, the top surface of the specimen was sprinkled with a small amount of fine sand; then, the specimen was placed on the loading plate of the PMS. According to the results of the UCS tests, the maximum load, which is generally 60% of the UCS value, was determined. The maximum load was divided into five portions equally and loaded sequentially. Each load was applied for 1 min, and then the displacement was recorded and the load was removed to recover the elastic deformation of the specimen. The displacement was recorded at 0.5 min of unloading and the second portion of the load was applied. Subsequent procedures were carried out accordingly until the resilient deformation under the last portion of the load was recorded. The CRM value is calculated according to the following equation.

$$E = \frac{ph}{l} \quad (5)$$

where  $E$  is CRM (MPa);  $P$  is the pressure (MPa);  $h$  is the height of the specimen (mm); and  $l$  is the resilience distortion of the specimen (mm).

## 4. Mix Design

### 4.1. Laboratory Gradation Design

The best physical and mechanical properties of LPS-GCSM are achieved when the gradation structure is skeleton-dense. Therefore, the maximum dry density of the mixture is taken as an indicator to evaluate the degree of void filling and to examine whether the gradation is in a dense condition, which ensures the durability of the mixture. At the same time, the deformation resistance of LPS-GCSM can be detected by the CBR test, where the CBR value shows the degree of mutual embedding of aggregates.

Six kinds of gradation were designed to optimize the gradation of LPS-GCSM in the test battery through laboratory compaction and the CBR test. Then, the gradation with superior maximum dry density and CBR values was selected as the target gradation after analyzing the test results. The aggregates used for the laboratory tests were divided into five sets, i.e., 1# (20–40 mm), 2# (20–30 mm), 3# (10–20 mm), 4# (5–10 mm), and 5# (0–5 mm). The sieve passing rates for each set are detailed in Table 4. The sieve passing rates for the six designed levels of gradation, named G1, G2, G3, G4, G5, and G6, are presented in Table 5. G1, G2, G3, and G4 are levels of gradation of LPS-GCSM, while G5 and G6 are levels of gradation of conventional GCS.

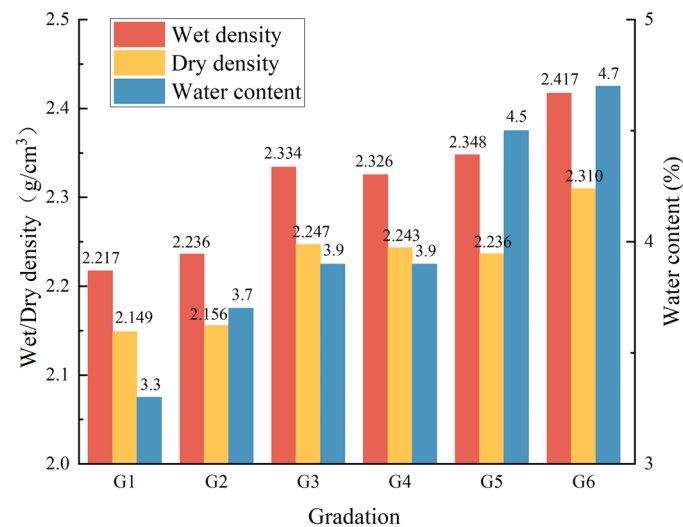
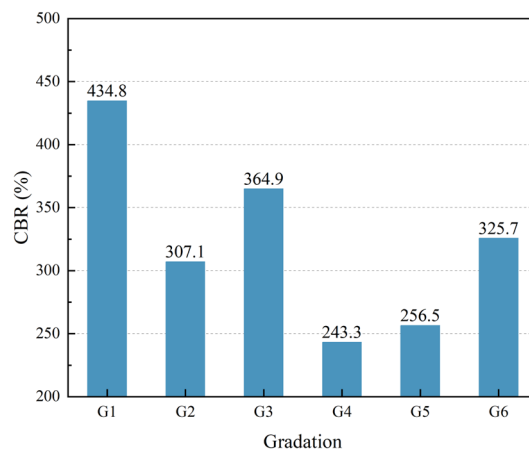
**Table 4.** The sieve passing rates for each set.

Set	Percentage of Mass Passing through the Following Sieve (%)														
	53	37.5	31.5	26.5	19.0	16.0	13.2	9.5	4.75	2.36	1.18	0.6	0.3	0.15	0.075
1#	100	72.3	25.5	6.3	0.3	0.3	0.3	0.3	0.3	0.3	0.3	0.2	0.2	0.2	0.2
2#	100	100	100	100	41.3	12.0	0.3	0.3	0.2	0.2	0.3	0.2	0.2	0.2	0.2
3#	100	100	100	100	54.8	26.4	8.6	0.8	0.2	0.2	0.2	0.2	0.2	0.2	0.2
4#	100	100	100	100	100	100	100	90.6	5.1	1.2	1.1	1.1	1.1	0.8	0.8
5#	100	100	100	100	100	100	100	100	92.0	65.7	50.2	36.8	23.8	8.5	7.6

The compaction and CBR test results of the six different levels of gradation of LPS-GCSM are shown in Figure 5 and Figure 6, respectively.

**Table 5.** The sieve passing rates for the designed six levels of gradation.

Gradation 1#: 2#: 3#: 4#: 5#	Percentage of Mass Passing through the Following Sieve (%)														
	53	37.5	31.5	26.5	19.0	16.0	13.2	9.5	4.75	2.36	1.18	0.6	0.3	0.15	0.075
G1 (55:0:15:8:22)	100	83.4	55.3	43.8	35.7	32.8	31.1	29.4	20.0	14.1	10.8	8.0	5.3	2.0	1.8
G2 (51:0:19:7:23)	100	85.3	60.5	50.4	41.8	38.3	36.2	34.3	23.7	16.7	12.8	9.5	6.2	2.3	2.1
G3 (44:0:20:10:26)	100	87.5	66.5	57.9	47.0	41.9	38.7	36.3	24.7	17.4	13.3	9.8	6.4	2.4	7.8
G4 (34:0:26:12:28)	100	92.5	79.9	74.7	60.4	52.5	47.5	43.7	26.8	18.7	14.4	10.6	7.0	2.6	2.4
G5 (0:45:0:25:30)	100	100	100	100	73.4	58.9	51.8	48.4	28.7	20.1	15.4	11.4	7.5	2.8	2.5
G6 (0:40:0:28:32)	100	100	100	100	76.0	63.0	56.6	53.2	31.6	22.0	16.9	12.5	8.2	3.1	2.8

**Figure 5.** The result of compaction tests.**Figure 6.** The result of CBR tests.

As can be seen from Figure 5, the maximum dry density values of LPS-GCSM are less than those of conventional GCS. The wet density also exhibits a similar trend. For G1, G2, G3, and G4, when the coarse aggregate content decreases and the fine aggregate content increases, the wet and dry densities and the optimum water contents of the specimens gradually increase. This is due to the fact that the increase in fine aggregate can fill up the voids of the coarse aggregate skeleton during the compaction process, so that the overall void ratio of the mixture is reduced, thus forming a tight skeleton-dense structure [41].

As shown in Figure 6, the CBR values of the LPS-GCSM designed in this paper can reach up to 434.8%. This is because the shear strength and load-bearing capacity of GCS

are increased as the maximum particle size increases. Due to the higher content of coarse aggregates in the mixture, the particles are also more likely to form a strong interlocking skeleton structure, and the overall strength and stiffness of the LPS-GCSM are consequently greater. Moreover, when the coarse aggregate content decreases and the fine aggregate content increases, the relationship between CBR and gradation of the specimens is not evident, but the overall tendency is decreasing. This indicates that LPS-GCSM has a better bearing capacity and deformation resistance when used as pavement base materials compared to conventional GCS.

In conclusion, the mixture with G3 gradation possesses a higher maximum dry density and CBR value, making it superior in terms of durability and bearing capacity. Therefore, G3 was selected as the target gradation.

#### 4.2. Field Gradation Design

Based on the laboratory gradation design, the raw material variation, mixing building performance, and field paving uniformity were considered to adjust the target gradation. Field LPS-GCSM was divided into four sets (shown in Table 6), which were 20–40 mm, 10–20 mm, 5–10 mm, and 0–5 mm. The aggregate sizes of these were combined at a ratio of 44:20:10:26, respectively. The levels of gradation are shown in Figure 7. The limitation of the gradation was according to the standard “Technical Specification for Construction of Large Size Graded Crushed Stone Base”.

**Table 6.** Four sets of field LPS-GCSM.

Set	Percentage of Mass Passing through the Following Sieve (%)													
	37.5	31.5	26.5	19	16	13.2	9.5	4.75	2.36	1.18	0.6	0.3	0.15	0.075
20–40 mm	82.0	47.0	14.7	0.6	0.1	0.1	0.1	0.1	0.1	0.0	0.1	0.0	0.0	0.0
10–20 mm	100	100	100	50.8	24.7	11.3	0.6	0.1	0.1	0.0	0.0	0.0	0.0	0.0
5–10 mm	100	100	100	100	100	100	77.2	3.0	1.0	0.6	0.6	0.6	0.6	0.6
0–5 mm	100	100	100	100	100	100	100	96.9	69.7	52.9	37.8	29.7	17.4	15.1

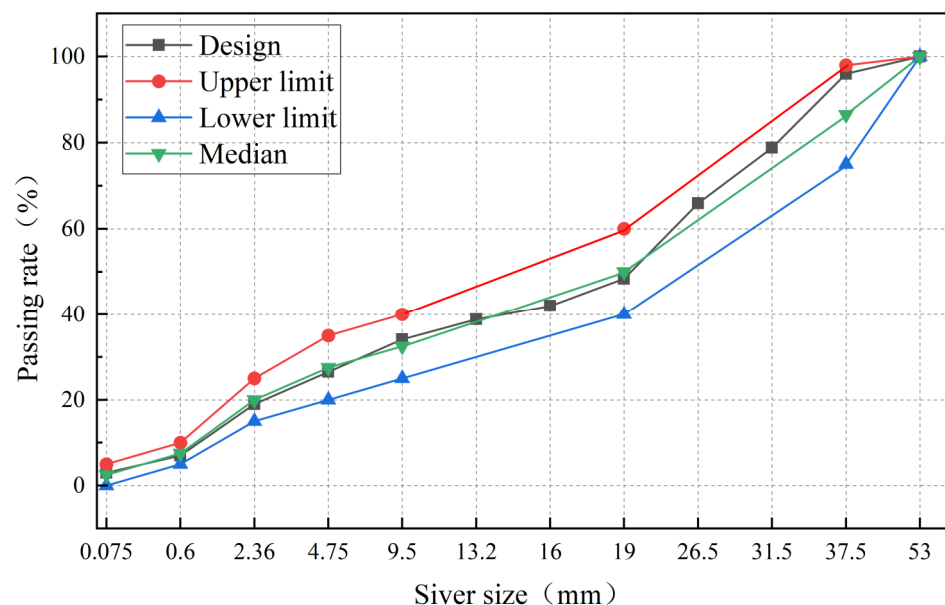


**Figure 7.** Levels of gradation.

As shown in Figure 7, the designed gradation presents an “S” shape, which is an interrupted gradation. The pass rates of 19 mm and 4.75 mm sieves are 48.4% and 26.5%, respectively, which are close to the median value of the designed gradation.

In the field trial paving, when the passing rates of 19 mm and 4.75 mm were close to 40% and 22%, respectively, which were close to the lower limit of the gradation, this resulted in more coarse aggregate after paving and obvious embedding and squeezing effects of the mixture. In addition, the homogeneity of the field-paved mixture was poor, with significant segregation. The coarse aggregates at the segregation were more easily crushed by steel wheel rollers. Therefore, it is recommended that the 19 mm and 4.75 mm passing rates should be approximately at the median value of the gradation, given considerations of field paving uniformity and the coarse aggregate embedding effect. The paving performance of the LPS-GCSM subbase in this study is presented in Figure 8a,b. As can be seen from the figures, the homogeneity of LPS-GCSM after field paving was satisfactory and no obvious segregation was observed.

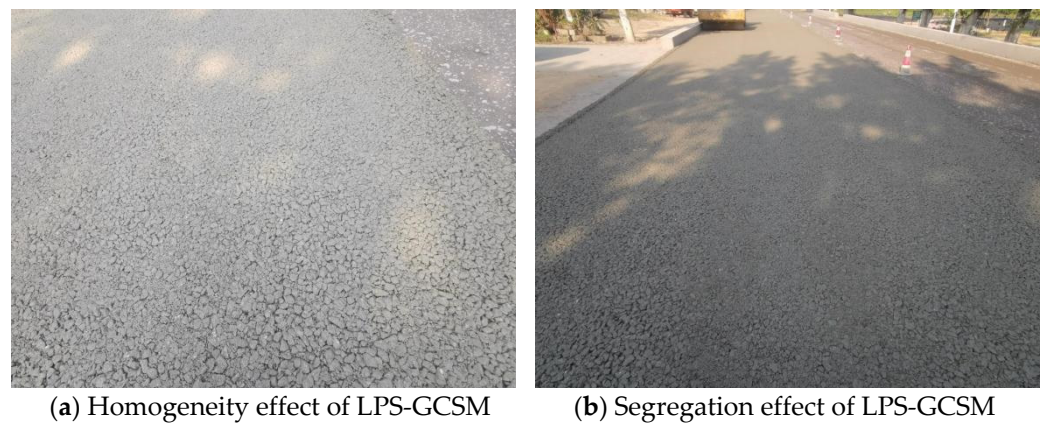


**Figure 8.** Paving performance of LPS-GCSM subbase.

### 5. Mechanical Properties of LCC-LPS-GCS

In order to improve the mechanical properties of LPS-GCSM, 2.5% cement was added to the mixture to form LCC-LPS-GCS. The results of the UCS and CRM tests of LCC-LPS-GCS are shown in Figure 9. The error bars mean the standard deviation of each dataset from the mean of group replicates [42].

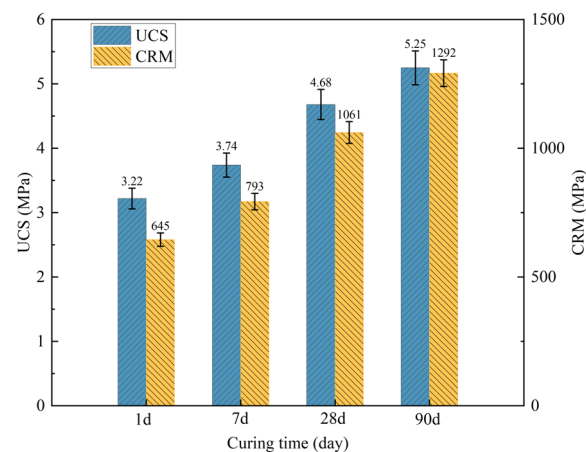


**Figure 9.** The results of the UCS and CRM tests.

As can be seen in Figure 5, both UCS and CRM gradually increase with the increase in curing time. The 7 days UCS is 3.74 MPa, which meets the requirements of the base layer and subbase course for second-class highways under heavy traffic (3.0–5.0 MPa and 2.0–4.0 MPa). During the period from 0 day to 28 days, the UCS and CRM values increase at a rapid rate, which slows after 28 days. This is because the cement hydration reaction is intense during the period from 0 day to 28 days, and the hydration products (C-S-H

cementitious materials) increase. Sufficient interaction between cement and aggregates occurs, which gradually strengthens the overall structure of the mixture. Thus, the UCS and CRM of the mixture increase fast. However, after 28 days, cement hydration has been completed, and the cement hydration rate slows, resulting in a slow increase. This trend is similar to that of cement-stabilized materials whose strength increases with curing time.

The CRM of LCC-LPS-GCS is higher than that of conventional GCS with the addition of same low-dose cement. This is because the CRM of the mixture is mainly determined by the modulus of the raw material and the structural form of the material composition. On the one hand, the modulus of the aggregate increases with the increase in particle size. LCC-LPS-GCS contains more large-particle-size aggregates, thus leading to an increase in the overall modulus of the mixture. On the other hand, the coarse aggregates of LCC-LPS-GCS are well interlocked and the fine aggregates filled the voids well, resulting in a tight skeleton-dense structure. In summary, the CRM of LCC-LPS-GCS is significantly higher than that of low-dose cement-modified conventional GCS.

## 6. Field Detection

Based on the results of the gradation design of LPS-GCSM and the mechanical properties of LCC-LPS-GCSM, a test road was paved to further examine the performance of the designed gradation. The test road comprises K 3744+900-K 3753+900 cement pavement rehabilitation and reconstruction engineering from Xindi to Niuling of the G207 line in Guangxi Zhuang Autonomous Region, China. The total length of the test road is about 9 km. The structure of the reconstructed pavement is illustrated in Figure 10.

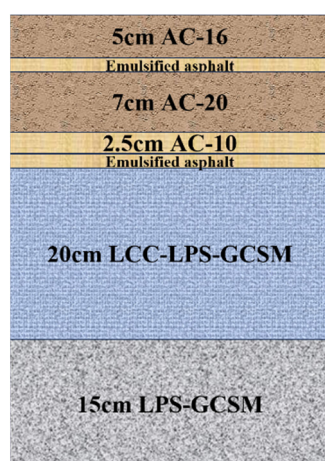


**Figure 10.** The structure of the reconstructed pavement.

### 6.1. Degree of Compaction

According to the Chinese specification JTG 3450-2019 [43], the field degree of compaction can be evaluated by the solid volume rate, which is required to be examined every 200 m. The compaction tests covered the entire test road, with a total of 45 detection points. The result for the solid volume rate should be higher than 85%. The field degrees of compaction of the base and subbase are shown in Figures 11 and 12, respectively. The dotted lines in the figures represent the average values.

From Figures 7 and 8, it can be seen that the compaction degree of the LPS-GCSM subbase of the test road is more than 97, and the compaction degree of the 2.5% low-dose cement-modified LPS-GCSM base is more than 98. Both of them met the specification requirements and showed satisfactory compaction effects. The thicknesses of the subbase and base course were maintained at 14–16 mm and 19–21 mm, respectively. This indicates that the gradation of the LPS-GCSM designed in this study is reasonable with the optimum water content to keep the mixture in a skeleton-dense condition. In addition, a combination of steel-wheel and rubber-wheel rollers was used for the rolling of the base and subbase. This method is effective in reducing the crushing of coarse aggregates, thus avoiding

changes to the original gradation of the mixture. At the same time, the traffic was not interrupted during construction, which allowed us to make full use of the traffic load on the mixture for the second compression. As a result, LPS-GCSM exhibits favorable compaction.

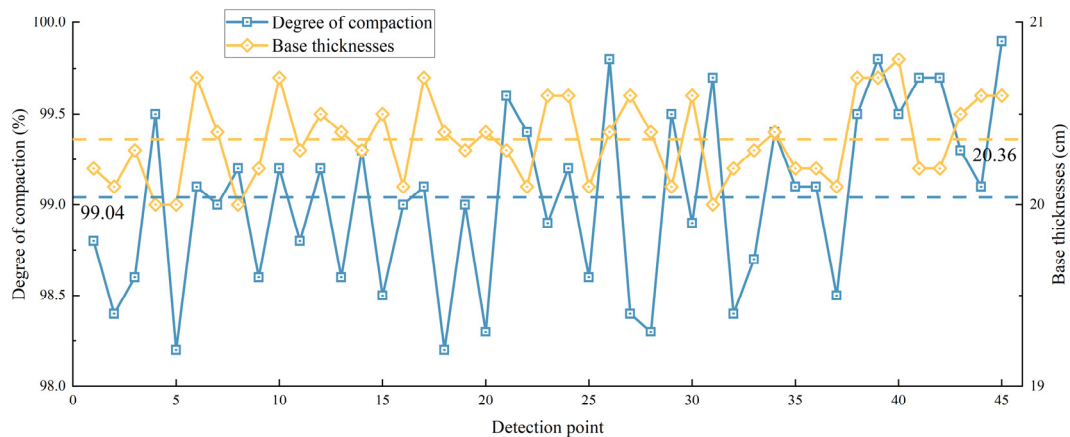


**Figure 11.** The degree of compaction of the base.

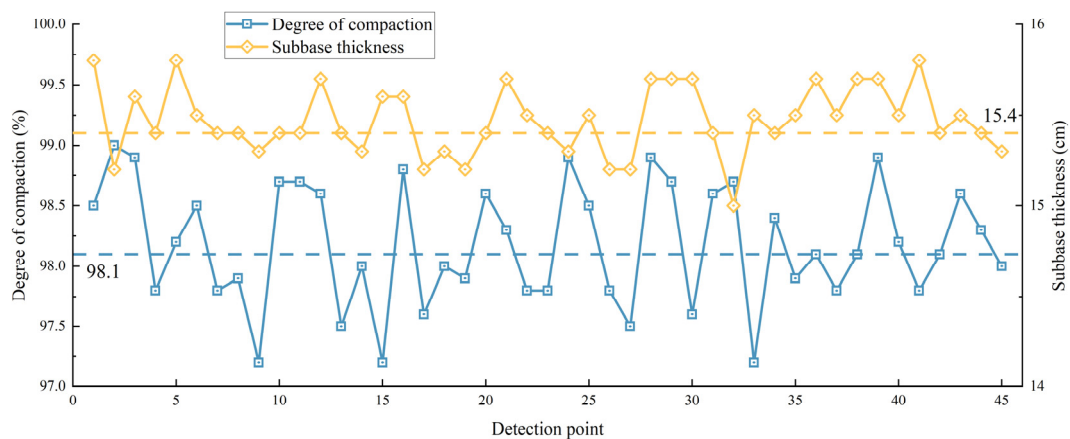


**Figure 12.** The degree of compaction of the subbase.

When comparing Figures 7 and 8, it can be seen that the average degree of compaction of the LCC-LPS-GCSM base is 0.86% higher than that of the LPS-GCSM subbase. This suggests that the addition of a low content of cement not only improves the mechanical properties of LPS-GCSM but also improves the degree of compaction appropriately. In addition, the variation in the degree of base compaction is 0.02% smaller than that of the subbase compaction. This indicates that the addition of cement also improves the stability of the field mixture compaction.

### 6.2. Deflection

Four sections (K 3745+200~K 3746+000, K 3746+000~K 3746+800, K 3748+500~K3749+300, and K 3752+700~K 3753+500) were selected from the test road for the detection of deflection. According to the Chinese specification JTG 3450-2019 [43], a Falling Weight Deflectometer (FWD) was used to test the deflection values. The field deflection test was conducted on the day before the upper course was paved. The frequency of the test was every 20 m. The results of the field deflection test are shown in Figure 13a–d. The dotted lines in the figures represent the average values. Representative values of deflection tests are summarized in the following Table 7.

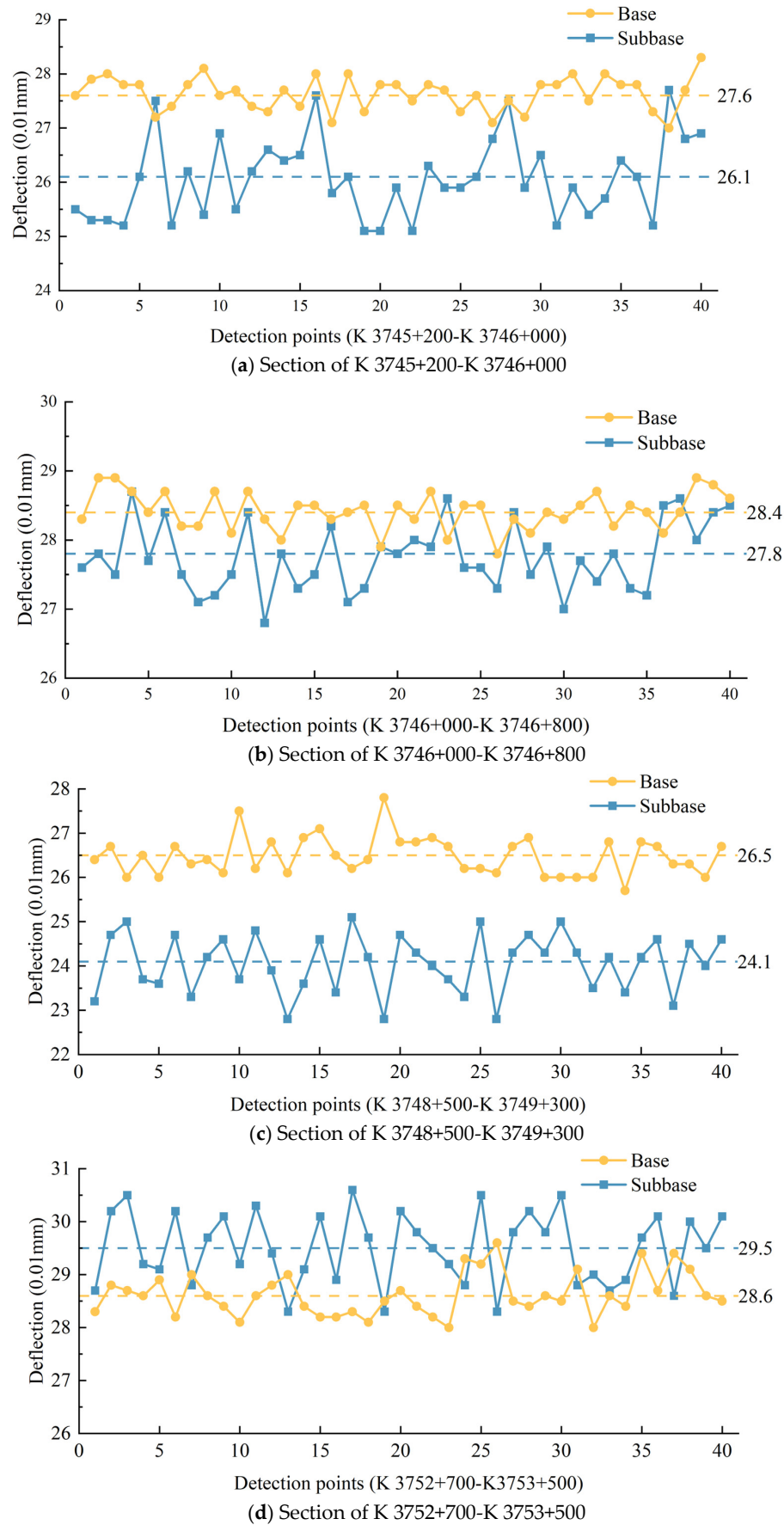


Figure 13. The results of deflection tests.

**Table 7.** Representative values of deflection tests.

Test Road Sections	Number of Detection Points	Representative Value of Subbase Deflection (0.01 mm)	Representative Value of Base Deflection (0.01 mm)
S1: K 3745+200- K 3746+000	40	27.6	26.1
S2: K 3746+000- K 3746+800	40	28.4	27.8
S3: K 3748+500- K 3749+300	40	26.5	24.1
S4: K 3752+700- K 3753+500	40	28.6	29.5

In Figure 9, the variance of base deflection values is less than that of subbase deflection values in the four sections of the test road. This suggests that the base will be subjected to more uniform stress when a course of LPS-GCSM is added between the old pavement and the LCC-LPS-GCSM base. In this way, the surface course of asphalt mixtures can be ensured to be uniformly stressed, which can reduce pavement damage. From Table 7, it can be observed that all representative values of deflection are less than 30 for both the base and subbase. This indicates that LPS-GCSM has excellent a load-bearing capacity as pavement structures. In addition, the deflection values of the subbase are smaller than those of the base except for the section S4. This demonstrates that the addition of a low content of cement can reduce the deflection of LPS-GCSM as pavement structures.

From the results of compaction and CBR field tests, it can be seen that the LPS-GCSM designed in this study is in a skeleton-dense state. The coarse aggregates of the mixture are mutually embedded and the fine aggregates fully fill the voids of the coarse aggregates, which exhibit an excellent load-bearing capacity and durability. Therefore, it is reasonable to adopt maximum dry density and CBR values as the gradation design indicators for LPS-GCSM.

## 7. Conclusions

According to the results of our tests and detection efforts, the main conclusions and recommendations are summarized in the following:

- (1) The optimum gradation of LPS-GCSM can be achieved by a combination of aggregate sizes of 20–40 mm, 10–20 mm, 5–10 mm, and 0–5 mm at a ratio of 44:20:10:26.
- (2) The passing rates of 19 mm and 4.75 mm of the mixture should be approximately at the median value of the gradation, given considerations of field paving uniformity and the coarse aggregate interlocking effect.
- (3) The UCS and CRM values of LCC-LPS-GCSM increase at a rapid rate from 0 day to 28 days, while slowing after 28 days, which is a similar trend to those of cement stabilized materials.
- (4) LPS-GCSM exhibits favorable compaction and the addition of cement also improves the stability of the field mixture's compaction. The CRM of LCC-LPS-GCS is significantly higher than that of low-dose cement-modified conventional GCS.
- (5) The addition of a subbase course of LPS-GCSM between the old pavement and the LCC-LPS-GCSM base can generate more uniform stress on the base, which leads to a decrease in the occurrence of pavement damage.

## 8. Limitations and Further Research

In this paper, the mix design and bearing property of LPS-GCSM were investigated. Subsequent studies should explore other pavement performance factors of LPS-GCSM such as the dynamic modulus, drying, and temperature shrinkage, which can provide theoretical bases for the promotion and application of LPS-GCSM in different areas. Moreover, the investigation of microstructures of LCC-LPS-GCSM is also necessary in order to reveal the strength development mechanism of LPS-GCSM.

**Author Contributions:** Q.Y.: Conceptualization, Project Administration, Resources, Writing—Original Draft; J.X.: Formal Analysis, Investigation, Methodology, Writing—Original Draft, Writing—Review and Editing; H.P.: Investigation; X.L. (Xinchao Lv): Investigation; K.X.: Investigation; X.L. (Xuelian Li): Conceptualization, Project Administration, Writing—Review and Editing. All authors have read and agreed to the published version of the manuscript.

**Funding:** This research was funded by 2022 Transportation Industry Key Science and Technology Projects List Project “Research on Design and Structural Parameters of Flexible Base Course with Interlocking Large Particle Size Graded Crushed Stone” (No. GGL-YH-063).

**Data Availability Statement:** Data are contained within the article.

**Conflicts of Interest:** Authors Haoyu Pan, Xinchao Lv and Kuiyuan Xiong are employed by the company Guangxi Transportation Science and Technology Group Co., Ltd. The remaining authors declare that the research was conducted in the absence of any commercial or financial relationships that could be construed as a potential conflict of interest.

## References

- Xu, G.; Chen, Z.; Li, X.; Lu, G.; Dong, D.; Liu, Z. Establishment of Control Standard for Plastic Deformation Performance of Graded Crushed Stone. *Constr. Build. Mater.* **2019**, *211*, 383–394. [[CrossRef](#)]
- Bai, H.; Li, R.; Hu, X.; Chen, F.; Liao, Z. Automated Shape Analysis and DEM Study on Graded Crushed Stone. *Adv. Mater. Sci. Eng.* **2021**, *2021*, e3463363. [[CrossRef](#)]
- Luan, Y.; Ma, Y.; Ma, T.; Xia, F. Investigation on the Effects of Physical Property and Stress State of Graded Crushed Stone on Resilient Modulus and Permanent Deformation. *Constr. Build. Mater.* **2023**, *400*, 132628. [[CrossRef](#)]
- Xu, G.; Chen, Z.; Li, X.; Lu, G.; Dong, D.; Liu, Z. Simple Prediction Model for Plastic Deformation of Graded Crushed Stone Base for Flexible Pavement. *Mater. Struct.* **2020**, *53*, 36. [[CrossRef](#)]
- Rahman, M.S.; Erlingsson, S. Predicting Permanent Deformation Behaviour of Unbound Granular Materials. *Int. J. Pavement Eng.* **2015**, *16*, 587–601. [[CrossRef](#)]
- Mneina, A.; Shalaby, A. Relating Gradation Parameters to Mechanical and Drainage Performance of Unbound Granular Materials. *Transp. Geotech.* **2020**, *23*, 100315. [[CrossRef](#)]
- Zhang, J.; Li, J.; Yao, Y.; Zheng, J.; Gu, F. Geometric Anisotropy Modeling and Shear Behavior Evaluation of Graded Crushed Rocks. *Constr. Build. Mater.* **2018**, *183*, 346–355. [[CrossRef](#)]
- Jiang, Y.; Ni, C.; Zhang, Y.; Yi, Y. Numerical Investigation of the Plastic Deformation Behaviour of Graded Crushed Stone. *PLoS ONE* **2021**, *16*, e0258113. [[CrossRef](#)]
- Liang, P.; Yang, Y.; Huang, H.; Liu, J.; Guo, N. Experimental Study on Fractal Characteristics of Particle Size Distribution by Repeated Compaction of Road Recycling Crushed Stone. *Appl. Sci.* **2022**, *12*, 10303. [[CrossRef](#)]
- Qamhia, I.I.A.; Chow, L.C.; Mishra, D.; Tutumluer, E. Dense-Graded Aggregate Base Gradation Influencing Rutting Model Predictions. *Transp. Geotech.* **2017**, *13*, 43–51. [[CrossRef](#)]
- Lima, C.; Motta, L. Study of Permanent Deformation and Granulometric Distribution of Graded Crushed Stone Pavement Material. *Procedia Eng.* **2016**, *143*, 854–861. [[CrossRef](#)]
- Zhang, P.; Liu, J.; Wu, Y.; Shi, J. Application of Graded Crushed Stone Base in Urban Road Asphalt Pavement. In *Infrastructure Sustainability Through New Developments in Material, Design, Construction, Maintenance, and Testing of Pavements, Proceedings of the 6th GeoChina International Conference on Civil & Transportation Infrastructures: From Engineering to Smart & Green Life Cycle Solutions, Nanchang, China, 19–21 July 2021*; Tapase, A., Lee, J., Zhang, L., Eds.; Springer International Publishing: Cham, Switzerland, 2021; pp. 11–20.
- Xu, Y. Shear Strength Silumation Test Method of Graded Broken Stone and Its Appliance. Ph.D. thesis, Chang’an University, Xi’an, China, 2012.
- Chen, L.; Yan, E.; Xu, J.; Ma, T.; Zeng, J.; Gong, Y. Research on Design Indicators for Graded Crushed Stone Mixture Based on Vibration Molding Method. *Adv. Mater. Sci. Eng.* **2020**, *2020*, 5179563. [[CrossRef](#)]
- Chen, D.; Li, Y.; Cao, X.; Wu, T.; Zhang, H.; Qiao, Z.; Fan, Z.; Nan, Y.; Niu, C.; Wang, X.; et al. Microscopic Mechanical Properties and Fabric Anisotropic Evolution Law of Open Graded Gravel Permeable Base under Dynamic Loading. *Constr. Build. Mater.* **2023**, *402*, 132948. [[CrossRef](#)]
- Tan, B.; Yang, T. Analysis on Deformation Rule of Large-Size Graded Crushed Stone under Cyclic Rotary Axial Compression. *J. Highw. Transp. Res. Dev.* **2021**, *38*, 19–27.
- Yuan, J.; Shao, M. Gradation Selection of Grade Broken Stone. *Highway* **2005**, 140–145.
- Vavrik, W.; Pine, W.; Carpenter, S. Aggregate Blending for Asphalt Mix Design: Bailey Method. *Transp. Res. Rec. J. Transp. Res. Board* **2002**, *1789*, 146–153. [[CrossRef](#)]
- Vavrik, W.R.; Huber, G. *Bailey Method for Gradation Selection in HMA Mixture Design*; Transportation Research Circular No. E-C044; Transportation Research Board: Washington, DC, USA, 2002.

20. Eustacchio, E.; Fritz, H. *Mechanical Tests for Bituminous Mixes-Characterization, Design and Quality Control: Proceedings of the Fourth International RILEM Symposium*; CRC Press: Boca Raton, FL, USA, 1990.
21. Tan, B.; Yang, T.; Qin, H.; Liu, Q. Laboratory Study on the Stability of Large-Size Graded Crushed Stone under Cyclic Rotating Axial Compression. *Materials* **2021**, *14*, 1584. [[CrossRef](#)]
22. Tan, B.; Guo, Z.; Ni, Q. Research on Mechanical Properties of Granite Graded Macadam with Large Grain Size. *J. China Foreign Highw.* **2020**, *40*, 229–234.
23. Luo, L. Development and Application of Large Particle Size Aggregate Interlocking Base Material. Master's Thesis, Beijing University of Civil Engineering and Architecture, Beijing, China, 2020.
24. Suo, Z.; Zha, W.; Nie, L.; Qi, K. Research on the Application of Large Particle Size Graded Gravel in Asphalt Pavement Base. *Highway* **2022**, *67*, 35–40.
25. Guo, Z.; Tan, B.; Yue, A. Testing of the Large Size Granite Gravel Gradation Selections. *Soil Eng. Found.* **2018**, *32*, 668–671.
26. Ding, X.; Gan, X.; Liu, Q.; Li, C. Research on the Gradation Design Method of Super Large Particle Size Gravel Base Based on Recycled Cementitious Materials. *Highway* **2023**, *68*, 42–49.
27. Yuan, G.; Zhang, J. Research on Mechanical Performance and Micro-Structural Characteristics for Large Graded Aggregates. *Constr. Build. Mater.* **2022**, *341*, 127860. [[CrossRef](#)]
28. Shi, H. Research on the Application Technology of Large Particle Size Graded Crushed Stone in the Reconstruction of Old Cement Pavement. *J. China Foreign Highw.* **2009**, *29*, 243–245.
29. Xia, C.; Tan, J. Study on the Application of Large Particle Size Gravel in Overhaul Engineering. *West. China Commun. Sci. Technol.* **2018**, 84–87. [[CrossRef](#)]
30. Long, H. Analysis of the Application Effect of Large Particle Size Graded Crushed Stone in the Modification and Upgrading of Road Networks. *West. China Commun. Sci. Technol.* **2020**, 55–58. [[CrossRef](#)]
31. Zhou, X.; Huang, B.; Zhang, D. Application of Large-Size Graded Gravel in Road Network Engineering. *West. China Commun. Sci. Technol.* **2017**, 27–30. [[CrossRef](#)]
32. *JTG E42-2005; Test Methods of Aggregate for Highway Engineering*. Research Institute of Highway Ministry of Transport: Beijing, China, 2005.
33. *JTG/T F20-2015; Technical Guidelines for Construction of Highway Roadbases*. Research Institute of Highway Ministry of Transport: Beijing, China, 2015.
34. *JTG 3420-2020; Test Methods of Cement and Concrete for Highway Engineering*. Research Institute of Highway Ministry of Transport: Beijing, China, 2020.
35. *JTG 3430-2020; Test Methods of Soils Highway Engineering*. Research Institute of Highway Ministry of Transport: Beijing, China, 2020.
36. Long, W.; Xie, X.; Hai, L. Influence of Laboratory Compaction Methods on Shear Performance of Graded Crushed Stone. *J. Mater. Civ. Eng.* **2011**, *23*, 1483–1487. [[CrossRef](#)]
37. Xie, K.; Chen, X.; Li, T.; Deng, Z.; Yao, J.; Tang, L. A Framework for Determining the Optimal Moisture Content of High-Speed Railway-Graded Aggregate Materials Based on the Lab Vibration Compaction Method. *Constr. Build. Mater.* **2023**, *392*, 131764. [[CrossRef](#)]
38. Ji, X.; Lu, H.; Dai, C.; Ye, Y.; Cui, Z.; Xiong, Y. Characterization of Properties of Soil–Rock Mixture Prepared by the Laboratory Vibration Compaction Method. *Sustainability* **2021**, *13*, 1239. [[CrossRef](#)]
39. Taskiran, T. Prediction of California Bearing Ratio (CBR) of Fine Grained Soils by AI Methods. *Adv. Eng. Softw.* **2010**, *41*, 886–892. [[CrossRef](#)]
40. *JTG E51-2009; Test Methods of Materials Stabilized with Inorganic Binders for Highway Engineering*. Research Institute of Highway Ministry of Transport: Beijing, China, 2009.
41. Jiang, X.; Qin, R.; Gao, W.; Sha, A.; Chang, M. Gradation Fractal Characteristic and Mechanical Indexes of Super Large Stone Asphalt Mixture. *J. Traffic Transp. Eng.* **2013**, *13*, 7–14.
42. Li, X.; Xu, J.; Tang, Z.; You, Z.; Diab, A. Macro- and Microscale Properties of Stone Mastic Asphalt Mixtures Containing Calcium Sulfate Whisker. *J. Mater. Civ. Eng.* **2024**, *36*, 04024164. [[CrossRef](#)]
43. *JTG 3450-2019; Field Test Methods of Highway Subgrade and Pavement*. Research Institute of Highway Ministry of Transport: Beijing, China, 2019.

**Disclaimer/Publisher's Note:** The statements, opinions and data contained in all publications are solely those of the individual author(s) and contributor(s) and not of MDPI and/or the editor(s). MDPI and/or the editor(s) disclaim responsibility for any injury to people or property resulting from any ideas, methods, instructions or products referred to in the content.